Relative Contributions of Atmospheric Energy Transport and Sea Ice Loss to the Recent Warm Arctic Winter

HYE-MI KIM

School of Marine and Atmospheric Sciences, Stony Brook University, State University of New York, Stony Brook, New York

BAEK-MIN KIM

Korea Polar Research Institute, Incheon, South Korea

(Manuscript received 9 March 2017, in final form 8 June 2017)

ABSTRACT

The relative contributions of atmospheric energy transport (via heat and moisture advection) and sea ice decline to recent Arctic warming were investigated using high-resolution reanalysis data up to 2017. During the Arctic winter, a variation of downward longwave radiation (DLR) is fundamental in modulating Arctic surface temperature. In the warm Arctic winter, DLR and precipitable water (PW) are increasing over the entire Arctic; however, the major drivers for such increases differ regionally. In areas such as the northern Greenland Sea, increasing DLR and PW are caused mainly by convergence of atmospheric energy transport from lower latitudes. In regions of maximum sea ice retreat (e.g., northern Barents–Kara Seas), continued sea ice melting from previous seasons drive the DLR and PW increases, consistent with the positive ice–insulation feedback. Distinct local feedbacks between open water and ice-retreat regions were further compared. In open water regions, a reduced ocean–atmosphere temperature gradient caused by atmospheric warming suppresses surface turbulent heat flux (THF) release from the ocean to the atmosphere; thus, surface warming cannot accelerate. Conversely, in ice-retreat regions, sea ice reduction allows the relatively warm ocean to interact with the colder atmosphere via surface THF release. This increases temperature and humidity in the lower troposphere consistent with the positive ice–insulation feedback. The implication of this study is that Arctic warming will slow as the open water fraction increases. Therefore, given sustained greenhouse warming, the roles of atmospheric heat and moisture transport from lower latitudes are likely to become increasingly critical in the future Arctic climate.

1. Introduction

The winter of 2015/16 was the warmest Arctic winter on record (Boisvert et al. 2016; Cullather et al. 2016; Overland and Wang 2016; Kim et al. 2017). The Arctic averaged surface temperature was more than 4°C higher than the climatological value in January–February 2016 (Overland and Wang 2016). In particular, over the Barents Sea, the winter mean surface temperature anomaly exceeded 10°C, and the sea ice concentration (SIC) was 20% lower than the climatology (Cullather et al. 2016). The warming trend in the Arctic, which is more than twice the warming trend of the global mean, is known as Arctic amplification (Serreze et al. 2009; Serreze and Barry 2011; Cohen et al. 2014; Cohen 2016). Such abnormal warming in the Arctic may influence the weather and associated high-impact extreme events over the globe (e.g., Cohen et al. 2014; Kim et al. 2014; Barnes and Screen 2015; Francis and Skific 2015; Kug et al. 2015), although the impact of Arctic amplification on global climate remains controversial.

Observations show that Arctic warming has been most rapid during winter when solar radiation is at its minimum level (e.g., Bekryaev et al. 2010; Screen and Simmonds 2010b). The recent winter Arctic warming was caused by a combination of many factors that included warming associated with greenhouse gas increase, sea ice loss, and energy transport by atmospheric

Denotes content that is immediately available upon publication as open access.

Corresponding author: Baek-Min Kim, bmkim@kopri.re.kr

DOI: 10.1175/JCLI-D-17-0157.1

and oceanic processes (e.g., Carmack and Melling 2011; Serreze and Barry 2011; Bintanja and van der Linden 2013; Pithan and Mauritsen 2014). Among the various mechanisms proposed in relation to these multiple factors, recent studies have addressed the role of downward longwave radiation (DLR) to Arctic warming (Francis and Hunter 2006; Graversen and Wang 2009; Graversen et al. 2011; D. Park et al. 2015; H. Park et al. 2015a,b; Burt et al. 2016; Gong et al. 2017). Not only the trend but also the interannual variation of DLR is largest during winter (H. Park et al. 2015b).

Several factors can affect the variability of DLR during winter. When SIC decreases in the previous summer and fall, extra energy can be stored within the ocean owing to surface–albedo feedback, which can be released to the atmosphere in the following winter (Francis and Hunter 2006; Serreze and Francis 2006; Serreze et al. 2009; Screen and Simmonds 2010b; Serreze and Barry 2011). Excessive evaporation from the ocean increases DLR and could warm the surface air temperature, which in turn melts the sea ice. The sea ice decline reduces the insulating effect, and it allows surface turbulent heat flux (THF) to enter the atmosphere, warming the air near the surface. This process is called ''positive ice–insulation feedback'' (Burt et al. 2016). It dominates the sea ice–albedo feedback mechanism (e.g., Vihma 2014) during the Arctic winter when the contribution of shortwave radiation is negligible (e.g., Bintanja and van der Linden 2013). This process may be the dominant contributor to the largest surface warming signal in the Barents–Kara Seas where the greatest decline in SIC and increase in DLR have been observed in the recent decade.

In addition to the effect of the local sea ice decline, approximately half the warming trend caused by enhanced DLR is driven by moisture and heat transport from lower latitudes (e.g., Woods et al. 2013; Liu and Barnes 2015; H. Park et al. 2015b; Woods and Caballero 2016). For example, studies have shown that the warming in winter 2015/16 was triggered by a single extreme storm event that transported heat and moisture into the Arctic (Boisvert et al. 2016; Cullather et al. 2016; Overland and Wang 2016; Kim et al. 2017). Woods and Caballero (2016) found that such an intrusion of moisture is critical to winter Arctic warming and that the increased number of extreme intrusion events can explain approximately 45% of the trend of surface air temperature in the Barents Sea. D. Park et al. (2015) also found that about half the warming trend in the Barents–Kara Seas could be attributed to increased DLR due to moisture flux from lower latitudes. During winter, the Arctic atmosphere is relatively dry; therefore, it is sensitive to the small changes in the amount of moisture that can significantly modify the DLR (Francis and Hunter 2006; Winton 2006; Graversen and Wang 2009; Ghatak and Miller 2013; D. Park et al. 2015; H. Park et al. 2015a,b). Therefore, in addition to the impact of sea ice decline, energy transport via atmospheric moisture and heat has played a critical role in the recent Arctic warming. While the influence of each process (atmospheric energy transport and sea ice decline) to the recent Arctic warming has been investigated in previous studies, their relative contributions have not been clearly addressed. Here, we consider these processes together to explain the recent warming over the Arctic.

Although the warming trend is apparent over the entire Arctic, the most rapid and significant changes have been observed over the Barents–Kara Seas (e.g., Serreze et al. 2009; Screen and Simmonds 2010a; Parkinson and Cavalieri 2012; H. Park et al. 2015a,b). The Barents–Kara Seas are characterized by a marginal sea ice zone with significant fractions of sea ice leads (Wang et al. 2016). Sea ice leads, which are narrow cracks in the ice, play an important role in the Arctic climate. Small changes in lead fractions modulate atmospheric temperature (e.g., Lüpkes et al. 2008) and accelerate sea ice decline via the sea ice–albedo feedback (e.g., Stroeve et al. 2012). Climatologically, in sea ice leads, the relatively warm ocean is exposed to the cold atmosphere and therefore, the ocean releases heat and moisture into the air via THF (e.g., Lüpkes et al. 2008; Screen and Simmonds 2010a; Marcq and Weiss 2012). As ocean temperature does not change significantly, a change of the overlying atmospheric temperature modulates the vertical temperature gradient between the ocean and overlying atmosphere and it plays an active role in THF variability (Sorokina et al. 2016). During relatively warmer Arctic winters, although the atmosphere–ocean vertical temperature gradient decreases, the total area of sea ice leads expands and the sea ice retreats; thus, sensible and latent heat releases increase. However, in the open water region where sea ice does not exist, the decrease of vertical temperature gradient during warm Arctic winter results in turbulent flux suppression; therefore, such processes cannot enhance the near-surface warming. It means that the Arctic warming might depend on the fraction of the ice-retreat region. By comparing simulations from phase 5 of the Coupled Model Intercomparison Project (CMIP5), a recent study by Yim et al. (2016) found that when the SIC reaches its marginal value (10%–20%) under greenhouse warming, the models no longer maintain the ice–insulation feedback, thus slowing the warming trend. This means that the processes and sensitivity of Arctic amplification for a given radiative

forcing may depend on the SIC amount or, in other words, the fraction of the ice-retreat region. The contrast in the local feedback between the open water and ice-retreat regions has been discussed briefly in previous studies using either reanalysis data up to 1997 (Deser et al. 2000) or future climate projections (Deser et al. 2010; Yim et al. 2016), but not in the context of the significant warming in the recent decades.

Details of the data and methodology are introduced in section 2. The roles of atmospheric energy (heat and moisture) transport and sea ice decline with regard to the recent warm Arctic winter are discussed in section 3. The effects of local feedback in the open water and ice-retreat regions are compared in section 4. A summary and discussion are presented in section 5.

2. Data

The European Centre for Medium-Range Weather Forecasts (ECMWF) interim reanalysis (ERA-Interim, hereinafter ERAI; Dee et al. 2011) data outperform other reanalysis products in the Arctic (Jakobson et al. 2012). The reanalysis-based SIC is independent of but consistent with that obtained from satellite-based data over the region of interest in this study (Sorokina et al. 2016). The ERAI datasets are retrieved on a $1° \times 1°$ (latitude by longitude) grid. The vertically integrated moisture flux ($\mathrm{kg\,m^{-1}\,s^{-1}}$) and heat flux ($\mathrm{W\,m^{-1}}$) are used to compare the horizontal moisture and sensible heat transport by advection. By multiplying the latent heat of vaporization ($L = 2.26 \times 10^6\,\mathrm{J\,kg^{-1}}$) by the moisture flux, the convergence of the moisture flux and heat flux possesses the same unit as energy flux ($\mathrm{W\,m^{-2}}$). Additional details of the ERAI data can be found in Berrisford et al. (2011). Surface temperature from the HadCRUT4 hybrid with University of Alabama in Huntsville (UAH) data (HadCRUT4-UAH; Cowtan and Way 2014) is also compared to validate the results of the ERAI 2-m temperature T_{2m}. All the presented results are analyzed in the Northern Hemisphere winter period from December to February (DJF) over the period from 1979/80 to 2016/17. The 2015/16 winter, for example, comprises December 2015 and January–February 2016. The 2016/17 winter comprises only December 2016 and January 2017 because of data availability.

3. Contribution of atmospheric energy transport and sea ice loss to warm Arctic winter

a. Surface warming and sea ice loss

To investigate the underlying processes during the warm Arctic winter, the warm Arctic years were selected based on the ERAI T_{2m}. Figure 1 shows the interannual change in the DJF mean T_{2m} and SIC anomaly (multiplied by -1) averaged over the Arctic (62°–90°N) from 1979/80 to 2016/17. The time series of the T_{2m} and the surface temperature of HadCRUT4-UAH match well with a correlation coefficient >0.9 (Fig. 1). The coolest winter (1997/98) has the highest SIC, whereas the extreme warm winters (2015/16 and 2016/17) show very low values of SIC. Both T_{2m} and SIC have substantial interannual variability over the entire period with significant trends after around 1997/98. Interestingly, the time series of T_{2m} and SIC (Fig. 1) are uncorrelated before 1995 (temporal correlation coefficient of 0.04), and the relationship between these two variables changes after 1996 with a temporal correlation coefficient of 0.9. Even after removal of the linear trend, the correlation coefficient after 1996 remains above 0.8. The change of the relationship between T_{2m} and SIC is likely due to the increased sensitivity of the SIC variability to the warmer air temperature (Jun et al. 2014, 2016).

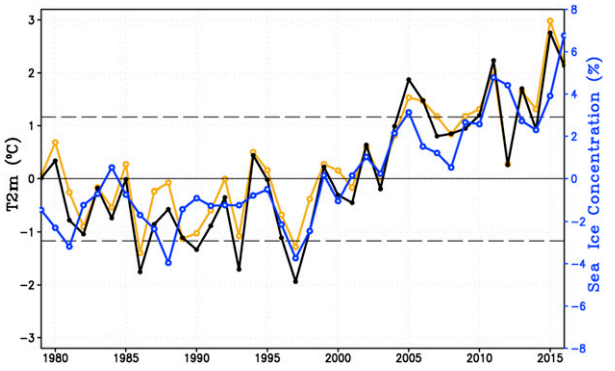

FIG. 1. Anomalous DJF mean T_{2m} (°C; black) and SIC (%; blue, multiplied by -1) averaged over 62°–90°N from 1979/80 to 2016/17. Surface temperature data from the HadCRUT4-UAH (yellow) are compared. Dashed horizontal lines indicate plus or minus one standard deviation of T_{2m}. Seven winters (2005/06, 2006/07, 2010/11, 2011/12, 2013/14, 2015/16, and 2016/17) are selected as warm Arctic winters.

A "warm Arctic year" is defined when the DJF mean T_{2m} (shown in Fig. 1) exceeds one standard deviation. Seven winters (2005/06, 2006/07, 2010/11, 2011/12, 2013/14, 2015/16, and 2016/17) are categorized as warm Arctic winters, all of which occurred after 2005. All the results shown here are based on the composites of these seven warm Arctic winters. A bootstrap technique (Efron 1979) was applied to determine the statistical significance of the composite anomalies. A composite anomaly for random Arctic winters was constructed with 7 years chosen at random with replacements from among the total 38 years. To obtain a probability distribution function, this process was repeated 10 000 times.

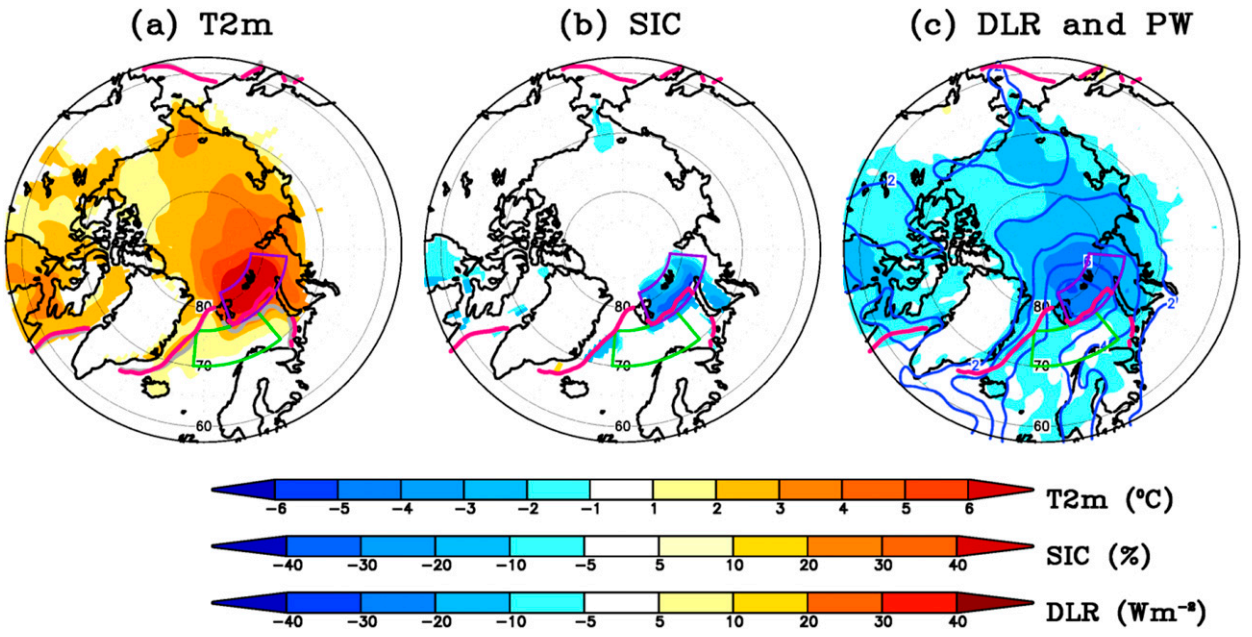

FIG. 2. Warm year composite of anomalous (a) T_{2m} (°C), (b) SIC (%), and (c) DLR (shading; W m^{-2}) and PW (blue contours, with 2 kg m^{-2} contour interval). Positive values for flux indicate upward. Only values exceeding 95% significance level are shaded in (a) and (b). Gray (magenta) contour indicates 15% SIC for climatology (warm Arctic years). Outlined boxes indicate the ice-retreat region (purple box; 76°–82°N, 20°–85°E) and open water region (green box; 70°–76°N, 5°W–40°E).

Figure 2 shows composites of the T_{2m}, SIC, DLR, and precipitable water (PW) anomalies in the warm Arctic years. The entire Arctic area is anomalously warm with a maximum of approximately 9°C in the Barents–Kara Seas (Fig. 2a). The gray and magenta lines (Fig. 2a) represent the 15% SIC line for the climatology and warm Arctic winters, respectively. In association with surface warming, a decrease of SIC of about 20%–30% is evident in the Barents–Kara Seas in the warm Arctic years (Fig. 2b). The northern Barents–Kara Seas in which SIC changed significantly is defined as the ''ice retreat'' region (Fig. 2, purple box). The southern part of the ice-retreat region is redefined as the ''open water'' region (Fig. 2, green box), which encompasses most of the southern Barents Sea as well as part of the northern Norwegian Sea and northern Greenland Sea. A clear distinction of the surface warming signal is evident to the south and north of the climatological 15% SIC line, which separates the ice-retreat and open water regions. In the open water region, surface warming is not as significant as in the ice-retreat region. While the open water region is generally not confined to such a small area, this region, which is adjacent to the ice-retreat region, was selected to compare the processes under relatively similar atmospheric conditions. Warming over the ice-retreat and open water regions appear to be driven by different processes (section 4).

The PW (Fig. 2c, blue contour), which reflects the vertically integrated water vapor, is increased over the entire Arctic region. Consistent with PW, enhanced DLR is also found over the entire Arctic (Fig. 2c; negative means downward). Here, enhanced DLR indicates greater downward radiation. The largest anomaly of approximately -30 W m^{-2} is observed over the northern Barents–Kara Seas. Similarities in the patterns between the DLR and PW suggest that DLR is strongly coupled with integrated water vapor during winter (e.g., Francis and Hunter 2007; Ghatak and Miller 2013). The temporal correlation between the interannual changes of winter mean DLR and PW averaged over the Arctic (62°–90°N) is 0.98. It should be emphasized that the surface warming and enhanced DLR and PW are observed over the entire Arctic during the warm Arctic winters.

b. *Atmospheric energy transport and ice–insulation feedback*

Climatologically, the transport of atmospheric moisture and heat from the North Atlantic into the Arctic is associated with the polar jet and storm tracks. To understand the contributions of atmospheric energy transport by horizontal moisture and heat advection to the recent Arctic warming, the spatial patterns of the anomalous heat and moisture fluxes in the warm Arctic years are compared in Fig. 3. Shadings represent the

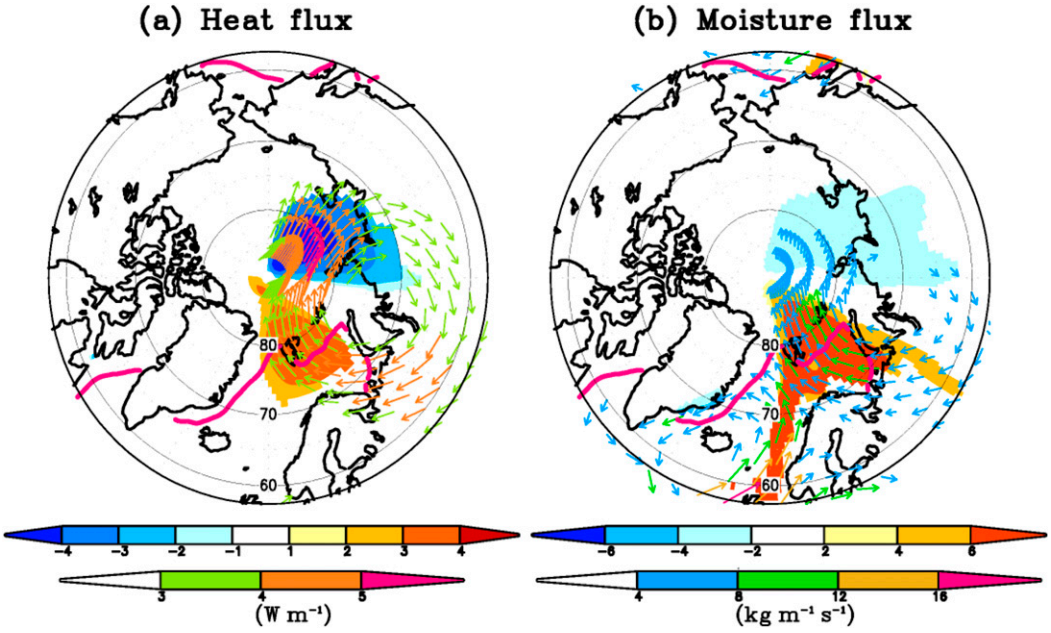

FIG. 3. As in Fig. 2, but for (a) vertically integrated meridional heat flux (shading; 10^9 W m^{-1}) and horizontal heat flux (vectors) and magnitude (vector color; 10^9 W m^{-1}) and (b) vertically integrated meridional moisture flux (shading; kg m^{-1} s^{-1}) and horizontal moisture flux (vectors) and magnitude (vector color; kg m^{-1} s^{-1}). Only values exceeding 90% significance level are shaded.

meridional components of the fluxes. The meridional transports of heat and moisture are considered as important sources for Arctic amplification (e.g., Woods et al. 2013; Woods and Caballero 2016; Kim et al. 2017). Strong poleward heat and moisture flux anomalies are evident from northern Europe toward the Arctic. Cyclonic (anticyclonic) flow anomalies to the west (east) are associated with anomalous poleward flux (Fig. 3). The temporal correlation coefficients between DLR and the poleward heat and moisture fluxes averaged over the northern European sector (70°–90°N, 0°–90°E) are −0.80 and −0.62, respectively (Table 1). It means that interannual changes in the heat and moisture transport from the northern European sector are linked to the modification of DLR.

Rather than the flux of heat and moisture, the convergence of these fluxes alters the atmospheric energy via thermal energy by temperature advection and via latent heat energy by latent heat release arising from condensation. Atmospheric thermal and latent heat energy are partly emitted toward the surface as DLR and they contribute to surface warming and sea ice melting. Also, enhanced humidity by moisture convergence increases the local greenhouse effect (e.g., Raval and Ramanathan 1989). Therefore, the convergence of both heat and moisture fluxes directly modulates DLR and near-surface temperature. Anomalous heat flux convergence is shown in the northern Greenland Sea where the maximum exceeds 80 W m^{-2} (Fig. 4a). The moisture flux convergence (Fig. 4b) is positive over most of the sea ice–covered area, except the Barents–Kara Seas, with substantial convergence in the northern Greenland Sea. The temporal correlation coefficient between the anomalous DLR (Fig. 2c) and heat

TABLE 1. Temporal correlation coefficient with DLR and variables over the 38-yr period. Variables include poleward moisture flux (VQ), poleward heat flux (VT), moisture flux convergence (VQconv), heat flux convergence (VTconv), SIC, LHF, and SHF. Variables are averaged over the northern European sector (70°–90°N, 0°–90°E), the ice-retreat region (76°–82°N, 20°–85°E), and the northern Greenland Sea (70°–90°N, 15°W–15°E, values marked with an asterisk). All values shown are statistically significant at the 99% confidence level.

	Northern European sector				Ice-retreat region			
	VQ	VT	VQconv	VTconv	SIC	LHF	SHF	SIC and LHF
DLR	−0.80	−0.62	−0.73*	−0.67*	0.83	−0.63	−0.49	−0.92

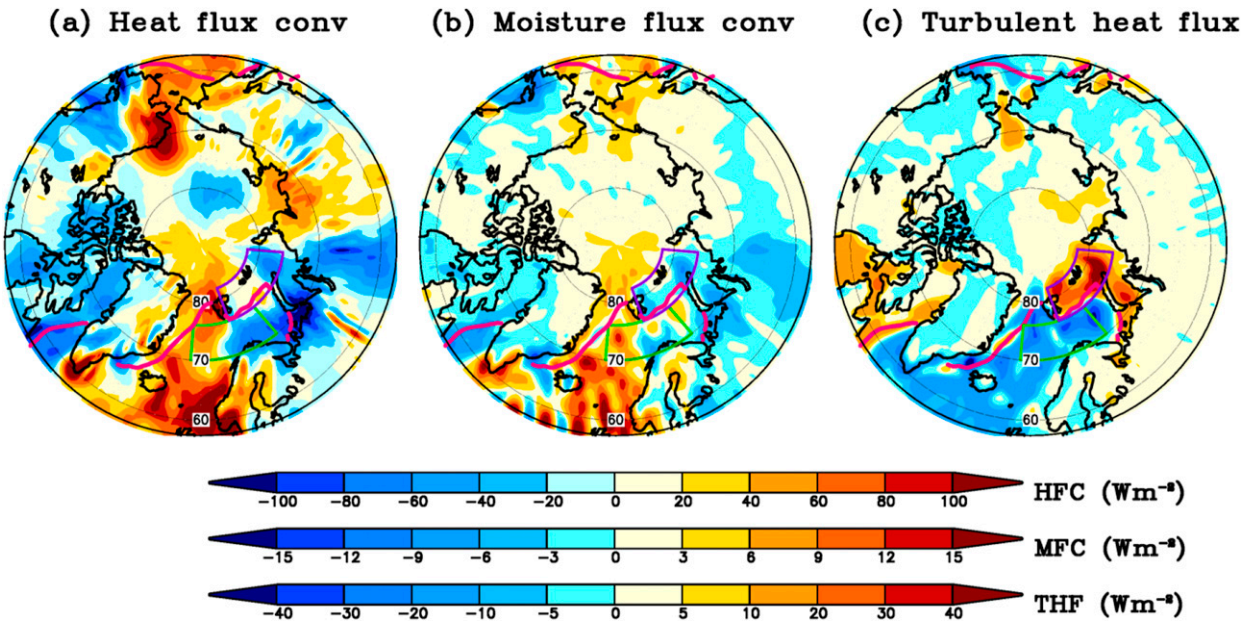

FIG. 4. As in Fig. 2, but for (a) vertical integral of heat flux convergence ($W\,m^{-2}$), (b) vertical integral of moisture flux convergence ($W\,m^{-2}$), and (c) THF ($W\,m^{-2}$). Positive values for surface fluxes indicate upward.

(moisture) flux convergence averaged over the northern Greenland Sea (70°–90°N, 15°W–15°E) is 0.67 (0.73) (Table 1). Overall, moisture flux convergence has a similar spatial pattern to heat flux convergence but it is one order of magnitude smaller (Fig. 4).

Over the ice-retreat region of the northern Barents–Kara Seas (purple box in Fig. 4), where SIC has the strongest decline and T_{2m} has the largest increase during the warm years (Fig. 2), both heat flux and moisture flux convergence are negligible. It indicates that the large DLR and PW anomalies over this region are not caused by atmospheric energy convergence but by other processes instead. It should be noted that this area is the largest ice-retreat region (Fig. 2b). Assuming that shortwave radiation is negligible in winter, the surface THF, which consists of sensible heat flux (SHF) and latent heat flux (LHF), contributes to the surface energy balance. Climatologically, because of the loss of energy from the relatively warmer ocean into the colder atmosphere, THF is always directed upward in the Arctic, except in regions entirely covered by thick ice where ocean–atmosphere interaction is weak. During the warm Arctic winters, the THF anomaly in the ice-retreat area shows strong upward flux with a maximum value of about $50\,W\,m^{-2}$ (Fig. 4c). Over the ice-retreat region, the THF likely declines over those regions where water was previously exposed, and the THF increases over newly open region, with net effect being an increase in the THF. The large THF anomaly is likely due to sea ice melting, which enables the ocean to interact with the atmosphere via THF release, thus contributing to the energy surplus of the atmosphere. Results indicate that, over the ice-retreat region where heat and moisture flux convergence is not significant, enhanced DLR and PW are likely the results of local THF release due to the sea ice melting. This, in turn, could contribute to the near-surface temperature increase and thus could maintain the ice–insulation feedback, although uncertainty remains whether this feedback is indeed taking place. The temporal correlation coefficients between the variables averaged over the ice-retreat region are compared in Table 1. The correlation coefficient between the DLR and SIC has a significant positive value ($r = 0.83$), meaning that the increase of DLR is associated with sea ice decline. The correlation between DLR and LHF (SHF) over the ice-retreat region is −0.63 (−0.49), meaning that the increase of DLR during the warm Arctic winters is mainly caused by the increase of evaporation as a result of sea ice melting (correlation between LHF and SIC is −0.92).

To recap briefly, it has been shown that increases of PW and DLR occur over the entire Arctic during the warm Arctic winters, but that their origins might be different. The increases of PW and DLR in some regions (e.g., northern Greenland Sea) are mainly caused by the convergence of the atmospheric energy transport from lower latitudes, while the increases of PW and DLR in ice-retreat regions (e.g., northern Barents–Kara Seas) are caused by continued SIC decline from the previous seasons/years. During the summer and fall prior to a

TABLE 2. Variables averaged over the open water (70°–76°N, 5°W–40°E), ice-retreat (76°–82°N, 20°–85°E), and ice-covered (70°–90°N, 85°E–0°) regions for climatology. Numbers in parentheses indicate anomalies in warm Arctic winter.

	Open water region		Ice-retreat region		Ice-covered region	
	Climatology	Warm year	Climatology	Warm year	Climatology	Warm year
T_{2m} (°C)	−2.1	−0.6 (1.5)	−17.4	−11.0 (6.4)	−27.0	−24.8 (2.2)
SST (°C)	3.0	3.6 (0.6)	−1.5	−1.4 (0.1)	−1.6	−1.6 (0.0)
ΔT (°C, SST − T_{2m})	5.1	4.2 (−0.9)	15.9	9.6 (−6.3)	25.4	23.2 (−2.2)
THF (W m^{-2})	148.3	132.5 (−15.8)	29.6	50.0 (20.4)	−3.8	−3.0 (0.8)

warm Arctic winter, a signal of SIC decrease already exists (not shown). As mentioned before, extra energy can be stored in the ocean, which provides favorable conditions for adding additional heat and water vapor directly into the atmosphere in the following winter (e.g., Ghatak and Miller 2013) and provides positive feedback for sea ice decline (e.g., Woods and Caballero 2016). While SIC decline is clearly observed in previous seasons, the patterns of the circulation in the previous seasons are completely different from those shown in winter (not shown). It indicates that the atmospheric circulation pattern is distinctive for warm Arctic winters and it is not a continuous phenomenon from previous seasons.

4. Distinct local feedback in open water versus ice-retreat region

The previous section showed that the major drivers for enhanced DLR and PW differ by region. One interesting feature observed in the T_{2m} composite (Fig. 2a) is that the temperature anomaly pattern shows a sharp contrast along the 15% SIC line that separates the ice-retreat and open water regions. Significantly large temperature anomalies are shown to the north of the 15% SIC line, while the signal eventually disappears to the south. This section compares the possible distinct local feedback mechanisms over the open water and ice-retreat regions that could be responsible.

During the warm Arctic winter, the dominant signals of increased atmospheric temperature and specific humidity are observed in the lower troposphere, making it a ''bottom-heavy'' atmospheric structure (Woods and Caballero 2016). Because of the warm and humid atmosphere, the gradients of temperature and water vapor pressure between the lower atmosphere and ocean surface decrease because ocean temperature does not change significantly. To understand the processes over the open water and ice-retreat regions, the sea surface temperature (SST), T_{2m}, and vertical temperature gradient between the ocean surface and lower atmosphere (ΔT = SST − T_{2m}) are compared (Table 2). Climatologically, in the open water region, ΔT is 5.1°C, indicating warmer SST (3.0°C) and colder T_{2m} (−2.1°C). Associated with the temperature gradient, about 148.3 W m^{-2} of THF is released from the ocean to the atmosphere in the open water region as a long-term average.

During warm Arctic winters, T_{2m} increases to −0.6°C, while the SST does not change significantly. This results in a decrease of ΔT from 5.1° to 4.2°C in the open water region. As the SST does not change much, warming of the overlying atmosphere plays an active role in the heat flux exchange. Associated with the reduced temperature gradient during warm Arctic winters, the THF is suppressed (Fig. 4c), which results in a decrease of 15.8 W m^{-2} in the open water region compared with the climatology. A significant fraction of the THF decrease is attributed to SHF reduction (−13.3 W m^{-2}), while the LHF reduction (−2.5 W m^{-2}) contributes <20% to the THF change. Therefore, THF does not support the warming of the lower atmosphere and surface warming cannot accelerate which is consistent with the results based on the CMIP5 models (Yim et al. 2016).

Over the ice-retreat region, the results are consistent with the positive ice–insulation feedback. Climatologically, the ice-retreat region is covered with >15% SIC, which results in a climatological value of THF (29.6 W m^{-2}) that is smaller than the open water region (148.3 W m^{-2}). During the warm Arctic years, although the temperature gradient ΔT decreases from 15.9° to 9.6°C, THF increases from 29.6 to 50.0 W m^{-2}, which is the opposite to the response in the open water region. Sea ice retreat causes excessive THF release, which can increase the temperature and humidity in the lower troposphere and thus could support maintaining the positive ice–insulation feedback. Therefore, it can be concluded that the sharp contrast of the warming signal shown in Fig. 2a is likely due to the change of SIC fraction in the sea ice retreat region where local feedback plays a significant role. We also compared the values in Table 2 for the sea ice–covered Arctic area (70°–90°N, 85°E–0°) which excludes the open water and ice-retreat region (Table 2). The increase of T_{2m} during the warm year over the ice-covered region (Fig. 2a and Table 2) is likely due to the increase of DLR (Fig. 2c),

which is caused by the horizontal heat flux and moisture convergence (Fig. 4). Although the T_{2m} increases during the warm year, the THF does not change significantly (Fig. 4c). This is likely due to the existence of thicker sea ice, which is less sensitivity to atmospheric variability than thinner ice.

5. Summary and discussion

Arctic warming has been most rapid during boreal winter when solar radiation is minimal. To understand the causes of the recent warm Arctic winters, the relative contributions of atmospheric energy transport (via heat and moisture advection) and sea ice decline have been investigated using high-resolution reanalysis data up to 2017. During warm Arctic winters, significant surface warming occurs, SIC declines, and DLR and PW increase over the Atlantic sector of the Arctic Ocean which includes the Greenland, Norwegian, Barents, and Kara Seas. However, the major drivers for the increases of DLR and PW differ by region. In some areas, such as the northern Greenland Sea, increases in DLR and PW are mainly caused by the convergence of atmospheric energy transport from lower latitudes, while in ice-retreat regions (e.g., northern Barents–Kara Seas) it is consistent with positive ice–insulation feedback by continued SIC decline from previous seasons. By considering these two effects (atmospheric energy transport and sea ice decline) together, the increases of DLR and PW and thus the surface temperature can be explained. However, many additional factors that might contribute to Arctic warming, such as ocean energy transport, have been excluded in this study and the impact of such factors warrants further study.

The local feedback mechanisms between the ice-retreat and open water regions were compared. In the open water region, a reduced temperature gradient suppresses THF release from the ocean to the atmosphere, meaning surface warming cannot accelerate. Conversely, over the ice-retreat region, sea ice melting allows the surface THF release, which can increase the temperature and humidity in the lower troposphere, consistent with the positive ice–insulation feedback. Therefore, local feedback may accelerate warming in ice-retreat regions, while it slows warming in open water regions, which results in the sharp contrast of the surface warming signals shown in Fig. 2a.

To summarize, this study showed that recent Arctic warming is caused not only by atmospheric energy transport from lower latitudes but also by continuous SIC decline. Full exploration of whether and by how much both the warming and the sea ice decline are caused by internal variabilities or by external forcing has not yet been undertaken; however, the trends of warming and sea ice decline during the past two decades are evident (Fig. 1). Whether these trends will remain stationary, accelerate, or decrease is an open question. This study has suggested that the rates of SIC decline and Arctic warming are likely to slow down as the fraction of open water region increases. This is consistent with a recent study by Yim et al. (2016), which showed that, in CMIP5 model simulations, Arctic warming tends to increase until SIC reaches a critical level of 10%–20%. After SIC reaches this critical level, the rates of Arctic warming and SIC decline no longer accelerate, even under the scenario of continued greenhouse warming (Yim et al. 2016). It means that, under the background of sustained greenhouse warming, the role of atmospheric heat and moisture transport from lower latitudes is likely to play an increasingly critical role in Arctic warming.

In warm Arctic winters, a wave pattern with strong poleward transport of moisture and heat from northern Europe to the Arctic is clearly observed (Fig. 3). However, it is unclear whether these poleward flux anomalies reflect a Rossby wave response caused by tropical forcing (e.g., Lee et al. 2011; Lee 2014), the North Atlantic Ocean (e.g., Sato et al. 2014; Ok et al. 2017), the Pacific decadal oscillation (e.g., Screen and Francis 2016), or unusual weather events such as the occurrence of extreme storm events (e.g., Woods and Caballero 2016; Kim et al. 2017) or any other factors. Moreover, the local changes of the fluxes in response to Arctic temperature change can act as a forcing for atmospheric circulation (e.g., Burt et al. 2016; Nakamura et al. 2016; Pedersen et al. 2016). Although all these factors can contribute to Arctic warming, separating their individual effects with observational data is difficult because of close coupling. Further understanding of the origins of the wave pattern and the associated processes warrants further study using numerical models; however, the simulations of Arctic temperature and sea ice by current numerical models are far from realistic (e.g., Chapman and Walsh 2007; Yim et al. 2016).

Acknowledgments. Constructive and valuable comments from three anonymous reviewers are greatly appreciated. This study was supported by the KMA R&D Program under Grant KMIPA 2016-6010 and project titled K-AOOS(KOPRI, PM17040) funded by the MOF, South Korea.

REFERENCES

Barnes, E. A., and J. A. Screen, 2015: The impact of Arctic warming on the midlatitude jet-stream: Can it? Has it? Will it? *Wiley Interdiscip. Rev. Climate Change*, **6**, 277–286, doi:10.1002/wcc.337.

Bekryaev, R. V., I. V. Polyakov, and V. A. Alexeev, 2010: Role of polar amplification in long-term surface air temperature variations and modern Arctic warming. *J. Climate*, **23**, 3888–3906, doi:10.1175/2010JCLI3297.1.

Berrisford, P., P. Kållberg, S. Kobayashi, D. Dee, S. Uppala, A. J. Simmons, P. Poli, and H. Sato, 2011: Atmospheric conservation properties in ERA-Interim. *Quart. J. Roy. Meteor. Soc.*, **137**, 1381–1399, doi:10.1002/qj.864.

Bintanja, R., and E. C. van der Linden, 2013: The changing seasonal climate in the Arctic. *Sci. Rep.*, **3**, 1556, doi:10.1038/srep01556.

Boisvert, L. N., A. A. Petty, and J. C. Stroeve, 2016: The impact of the extreme winter 2015/16 Arctic cyclone on the Barents–Kara Seas. *Mon. Wea. Rev.*, **144**, 4279–4287, doi:10.1175/MWR-D-16-0234.1.

Burt, M. A., D. A. Randall, and M. D. Branson, 2016: Dark warming. *J. Climate*, **29**, 705–719, doi:10.1175/JCLI-D-15-0147.1.

Carmack, E., and H. Melling, 2011: Cryosphere: Warmth from the deep. *Nat. Geosci.*, **4**, 7–8, doi:10.1038/ngeo1044.

Chapman, W. L., and J. E. Walsh, 2007: Simulations of Arctic temperature and pressure by global coupled models. *J. Climate*, **20**, 609–632, doi:10.1175/JCLI4026.1.

Cohen, J., 2016: An observational analysis: Tropical relative to Arctic influence on mid-latitude weather in the era of Arctic amplification. *Geophys. Res. Lett.*, **43**, 5287–5294, doi:10.1002/2016GL069102.

——, and Coauthors, 2014: Recent Arctic amplification and extreme mid-latitude weather. *Nat. Geosci.*, **7**, 627–637, doi:10.1038/ngeo2234.

Cowtan, K., and R. G. Way, 2014: Coverage bias in the HadCRUT4 temperature series and its impact on recent temperature trends. *Quart. J. Roy. Meteor. Soc.*, **140**, 1935–1944, doi:10.1002/qj.2297.

Cullather, R. I., Y.-K. Lim, L. N. Boisvert, L. Brucker, J. N. Lee, and S. M. J. Nowicki, 2016: Analysis of the warmest Arctic winter, 2015–2016. *Geophys. Res. Lett.*, **43**, 10 808–10 816, doi:10.1002/2016GL071228.

Dee, D. P., and Coauthors, 2011: The ERA-Interim reanalysis: Configuration and performance of the data assimilation system. *Quart. J. Roy. Meteor. Soc.*, **137**, 553–597, doi:10.1002/qj.828.

Deser, C., J. E. Walsh, and M. S. Timlin, 2000: Arctic sea ice variability in the context of recent atmospheric circulation trends. *J. Climate*, **13**, 617–633, doi:10.1175/1520-0442(2000)013<0617:ASIVIT>2.0.CO;2.

——, R. Tomas, M. Alexander, and D. Lawrence, 2010: The seasonal atmospheric response to projected Arctic sea ice loss in the late twenty-first century. *J. Climate*, **23**, 333–351, doi:10.1175/2009JCLI3053.1.

Efron, B., 1979: Bootstrap methods: Another look at the jackknife. *Ann. Stat.*, **7**, 1–26, doi:10.1214/aos/1176344552.

Francis, J. A., and E. Hunter, 2006: New insight into the disappearing Arctic sea ice. *Eos, Trans. Amer. Geophys. Union*, **87**, 509–511, doi:10.1029/2006EO460001.

——, and ——, 2007: Drivers of declining sea ice in the Arctic winter: A tale of two seas. *Geophys. Res. Lett.*, **34**, L17503, doi:10.1029/2007GL030995.

——, and N. Skific, 2015: Evidence linking rapid Arctic warming to mid-latitude weather patterns. *Philos. Trans. Roy. Soc.*, **373A**, 20140170, doi:10.1098/rsta.2014.0170.

Ghatak, D., and J. Miller, 2013: Implications for Arctic amplification of changes in the strength of the water vapor feedback. *J. Geophys. Res.*, **118**, 7569–7578, doi:10.1002/jgrd.50578.

Gong, T., S. Feldstein, and S. Lee, 2017: The role of downward infrared radiation in the recent Arctic winter warming trend. *J. Climate*, **30**, 4937–4949, doi:10.1175/JCLI-D-16-0180.1.

Graversen, R. G., and M. Wang, 2009: Polar amplification in a coupled climate model with locked albedo. *Climate Dyn.*, **33**, 629–643, doi:10.1007/s00382-009-0535-6.

——, T. Mauritsen, S. Drijfhout, M. Tjernström, and S. Mårtensson, 2011: Warm winds from the Pacific caused extensive Arctic sea-ice melt in summer 2007. *Climate Dyn.*, **36**, 2103–2112, doi:10.1007/s00382-010-0809-z.

Jakobson, E., T. Vihma, T. Palo, L. Jakobson, H. Keernik, and J. Jaagus, 2012: Validation of atmospheric reanalyses over the central Arctic Ocean. *Geophys. Res. Lett.*, **39**, L10802, doi:10.1029/2012GL051591.

Jun, S.-Y., C.-H. Ho, B.-M. Kim, and J.-H. Jeong, 2014: Sensitivity of Arctic warming to sea surface temperature distribution over melted sea-ice region in atmospheric general circulation model experiments. *Climate Dyn.*, **42**, 941–955, doi:10.1007/s00382-013-1897-3.

——, ——, J.-H. Jeong, Y.-S. Choi, and B.-M. Kim, 2016: Recent changes in winter Arctic clouds and their relationships with sea ice and atmospheric conditions. *Tellus*, **68A**, 29130, doi:10.3402/tellusa.v68.29130.

Kim, B.-M., S.-W. Son, S.-K. Min, J.-H. Jeong, S.-J. Kim, X. Zhang, T. Shim, & J.-H. Yoon, 2014: Weakening of the stratospheric polar vortex by Arctic sea-ice loss. *Nat. Commun.*, **5**, 4646, doi:10.1038/ncomms5646.

——, and Coauthors, 2017: Major cause of unprecedented Arctic warming in January 2016: Critical role of an Atlantic windstorm. *Sci. Rep.*, **7**, 40051, doi:10.1038/srep40051.

Kug, J.-S., J.-H. Jeong, Y.-S. Jang, B.-M. Kim, C. K. Folland, S.-K. Min, and S.-W. Son, 2015: Two distinct influences of Arctic warming on cold winters over North America and East Asia. *Nat. Geosci.*, **8**, 759–762, doi:10.1038/ngeo2517.

Lee, S., 2014: A theory for polar amplification from a general circulation perspective. *Asia-Pac. J. Atmos. Sci.*, **50**, 31–43, doi:10.1007/s13143-014-0024-7.

——, T. Gong, N. Johnson, S. B. Feldstein, and D. Pollard, 2011: On the possible link between tropical convection and the Northern Hemisphere Arctic surface air temperature change between 1958 and 2001. *J. Climate*, **24**, 4350–4367, doi:10.1175/2011JCLI4003.1.

Liu, C., and E. A. Barnes, 2015: Extreme moisture transport into the Arctic linked to Rossby wave breaking. *J. Geophys. Res.*, **120**, 3774–3788, doi:10.1002/2014JD022796.

Lüpkes, C., V. M. Gryanik, B. Witha, M. Gryschka, S. Raasch, and T. Gollnik, 2008: Modeling convection over Arctic leads with LES and a non-eddy-resolving microscale model. *J. Geophys. Res.*, **113**, C09028, doi:10.1029/2007JC004099.

Marcq, S., and J. Weiss, 2012: Influence of sea ice lead-width distribution on turbulent heat transfer between the ocean and the atmosphere. *Cryosphere*, **6**, 143–156, doi:10.5194/tc-6-143-2012.

Nakamura, T., K. Yamazaki, K. Iwamoto, M. Honda, Y. Miyoshi, Y. Ogawa, Y. Tomikawa, and J. Ukita, 2016: The stratospheric pathway for Arctic impacts on midlatitude climate. *Geophys. Res. Lett.*, **43**, 3494–3501, doi:10.1002/2016GL068330.

Ok, J., M.-K. Sung, K. Sato, Y.-K. Lim, S.-J. Kim, E.-H. Baik, and B.-M. Kim, 2017: How does the SST variability over the western North Atlantic Ocean control Arctic warming over the Barents–Kara Seas? *Environ. Res. Lett.*, **12**, 034021, doi:10.1088/1748-9326/aa5f3b.

Overland, J. E., and M. Wang, 2016: Recent extreme Arctic temperatures are due to a split polar vortex. *J. Climate*, **29**, 5609–5616, doi:10.1175/JCLI-D-16-0320.1.

Park, D.-S. R., S. Lee, and S. B. Feldstein, 2015: Attribution of the recent winter sea ice decline over the Atlantic sector of the Arctic Ocean. *J. Climate*, **28**, 4027–4033, doi:10.1175/JCLI-D-15-0042.1.

Park, H.-S., S. Lee, Y. Kosaka, S.-W. Son, and S.-W. Kim, 2015a: The impact of Arctic winter infrared radiation on early summer sea ice. *J. Climate*, **28**, 6281–6296, doi:10.1175/JCLI-D-14-00773.1.

——, ——, S.-W. Son, S. B. Feldstein, and Y. Kosaka, 2015b: The impact of poleward moisture and sensible heat flux on Arctic winter sea ice variability. *J. Climate*, **28**, 5030–5040, doi:10.1175/JCLI-D-15-0074.1.

Parkinson, C. L., and D. J. Cavalieri, 2012: Antarctic sea ice variability and trends, 1979–2010. *Cryosphere*, **6**, 871–880, doi:10.5194/tc-6-871-2012.

Pedersen, R. A., I. Cvijanovic, P. L. Langen, and B. M. Vinther, 2016: The impact of regional Arctic sea ice loss on atmospheric circulation and the NAO. *J. Climate*, **29**, 889–902, doi:10.1175/JCLI-D-15-0315.1.

Pithan, F., and T. Mauritsen, 2014: Arctic amplification dominated by temperature feedbacks in contemporary climate models. *Nat. Geosci.*, **7**, 181–184, doi:10.1038/ngeo2071.

Raval, A., and V. Ramanathan, 1989: Observational determination of the greenhouse effect. *Nature*, **342**, 758–761, doi:10.1038/342758a0.

Sato, K., J. Inoue, and M. Watanabe, 2014: Influence of the Gulf Stream on the Barents Sea ice retreat and Eurasian coldness during early winter. *Environ. Res. Lett.*, **9**, 084009, doi:10.1088/1748-9326/9/8/084009.

Screen, J. A., and I. Simmonds, 2010a: Increasing fall–winter energy loss from the Arctic Ocean and its role in Arctic temperature amplification. *Geophys. Res. Lett.*, **37**, L16707, doi:10.1029/2010GL044136.

——, and ——, 2010b: The central role of diminishing sea ice in recent Arctic temperature amplification. *Nature*, **464**, 1334–1337, doi:10.1038/nature09051.

——, and J. A. Francis, 2016: Contribution of sea-ice loss to Arctic amplification is regulated by Pacific Ocean decadal variability. *Nat. Climate Change*, **6**, 856–860, doi:10.1038/nclimate3011.

Serreze, M. C., and J. A. Francis, 2006: The Arctic on the fast track of change. *Weather*, **61**, 65–69, doi:10.1256/wea.197.05.

——, and R. G. Barry, 2011: Processes and impacts of Arctic amplification: A research synthesis. *Global Planet. Change*, **77**, 85–96, doi:10.1016/j.gloplacha.2011.03.004.

——, A. P. Barrett, J. C. Stroeve, D. N. Kindig, and M. M. Holland, 2009: The emergence of surface-based Arctic amplification. *Cryosphere*, **3**, 11–19, doi:10.5194/tc-3-11-2009.

Sorokina, S. A., C. Li, J. J. Wettstein, and N. G. Kvamstø, 2016: Observed atmospheric coupling between Barents Sea ice and the warm-Arctic cold-Siberian anomaly pattern. *J. Climate*, **29**, 495–511, doi:10.1175/JCLI-D-15-0046.1.

Stroeve, J. C., M. C. Serreze, M. M. Holland, J. E. Kay, J. Malanik, and A. P. Barrett, 2012: The Arctic's rapidly shrinking sea ice cover: A research synthesis. *Climatic Change*, **110**, 1005–1027, doi:10.1007/s10584-011-0101-1.

Vihma, T., 2014: Effects of Arctic sea ice decline on weather and climate: A review. *Surv. Geophys.*, **35**, 1175–1214, doi:10.1007/s10712-014-9284-0.

Wang, Q., S. Danilov, T. Jung, L. Kaleschke, and A. Wernecke, 2016: Sea ice leads in the Arctic Ocean: Model assessment, interannual variability and trends. *Geophys. Res. Lett.*, **43**, 7019–7027, doi:10.1002/2016GL068696.

Winton, M., 2006: Does the Arctic sea ice have a tipping point? *Geophys. Res. Lett.*, **33**, L23504, doi:10.1029/2006GL028017.

Woods, C., and R. Caballero, 2016: The role of moist intrusions in winter Arctic warming and sea ice decline. *J. Climate*, **29**, 4473–4485, doi:10.1175/JCLI-D-15-0773.1.

——, ——, and G. Svensson, 2013: Large-scale circulation associated with moisture intrusions into the Arctic during winter. *Geophys. Res. Lett.*, **40**, 4717–4721, doi:10.1002/grl.50912.

Yim, B. Y., H. S. Min, B.-M. Kim, J.-H. Jeong, and J.-S. Kug, 2016: Sensitivity of Arctic warming to sea ice concentration. *J. Geophys. Res. Atmos.*, **121**, 6927–6942, doi:10.1002/2015JD023953.